Distance-Aware Bandwidth-Adaptive Resource Allocation for Wireless Systems in the Terahertz Band

Chong Han, *Member, IEEE*, and Ian F. Akyildiz, *Fellow, IEEE*

***Abstract*—Terahertz (0.06–10 THz) band communication is envisioned as a key technology to satisfy the increasing demand for ultrahigh-speed wireless links. In this paper, a distance-aware bandwidth-adaptive resource allocation scheme is developed for THz band communication networks, which has the objective to improve the distance. The proposed scheme captures the unique channel peculiarities including the relationship between the distance and the bandwidth, and strategically utilizes the spectrum to enable multiple ultrahigh-speed links. Based on the developed scheme, the subwindows of the THz spectrum, the modulations, and the transmit power are adaptively allocated, for both single-user and multiuser communications. The numerical results show that the developed resource allocation scheme improves the distances and exploitation of the THz spectrum significantly. Specifically, 10 Gb/s can be supported at 4 m in the multipath channel, while 100 Gb/s is achieved up to 21 m in the line-of-sight transmission with the use of 20 dB gain antennas. Furthermore, in the multiuser network, 14 10 Gb/s links can be supported simultaneously in the multipath channel. With the use of 20 dB gain antennas, 13 100 Gb/s links can be supported at the same time. Moreover, the developed resource allocation scheme outperforms the existing millimeter-wave systems and the nonadaptive scheme. This paper achieves the design objective and contributes to enable multiple ultrahigh-speed links in the THz band communication network.**

***Index Terms*—Bandwidth (BW)-adaptive, distance-aware, resource allocation, strategic spectrum allocation, terahertz (THz) band.**

I. Introduction

In recent years, the wireless data traffic grew exponentially, further accompanied by an increasing demand for higher data rates. The data rates have doubled every 18 months over the last three decades and are currently approaching the capacity of wireless communication systems [2]. Following this trend, the ultrahigh-speed data rates are expected to reach 100 Gigabit-per-second (Gb/s) or more within the next decade. New spectral bands as well as advanced physical layer solutions are required to support this high data rate for future wireless communications. In addition to many proposed solutions for next-generation advanced cellular systems [3], the (0.06–10) terahertz (THz) band is identified as one of the promising spectrum bands to enable ultrahigh-speed communications [4], [5].

For the realization of ultrahigh-speed wireless communication networks in the THz band, it is imperative to develop a novel communication scheme that can address the unique challenges and requirements, which are summarized as follows. First, the transmission distance for ultrahigh-speed communication is very limited due to the very high path loss. An advanced communication scheme needs to be developed with the object to improve the transmission distance to support single or even multiple ultrahigh-speed links simultaneously [6]. Second, the physical properties in the channel need to be taken into account. For example, the very strong relationship between the distance and the bandwidth (BW) in the THz band requires adaption of the utilized BW as a function of the distance. Moreover, the delay spread and the coherence BW [7] affect the physical parameters design in the communication scheme. Third, the enormous usable BW in the THz band needs to be fully and efficiently exploited in multiuser networks. In particular, a strategic spectrum utilization design is demanded to simultaneously support multiple ultrahigh-speed links in the THz band.

In light of these challenges, the development of a resource allocation scheme appears to be attractive, which have been well investigated for the multiuser multicarrier systems at lower frequencies [8]–[12]. However, none of these existing works fully addresses the aforementioned challenges. Recently, ultrahigh-speed communication schemes in the THz band have been studied. For example, a single-band pulse-based scheme was proposed in [13]. Moreover, a multiwideband waveform design was analyzed in [14], in which an optimization framework is formulated to solve for the transmit power and the number of frames, with the aim to maximize the distance. Nevertheless, these two schemes rely on pulse-based communications and do not support more spectrum-efficient modulations, which poses a limitation on the maximum achievable data rates. Furthermore, experimental studies in [15]–[17] have shown the feasibility of broadband communications by exploiting the low THz frequencies (i.e., around 0.3 THz) to enable 100 Gb/s wireless links below 20 m. However, the resources including the ultrabroad BW, the modulation scheme, and the transmit power are not jointly and intelligently utilized, by being aware of the distance-BW dependence in the THz band.

Manuscript received September 23, 2015; revised February 15, 2016; accepted May 11, 2016. Date of publication June 13, 2016; date of current version July 08, 2016. This work was supported by the U.S. National Science Foundation under Grant ECCS-1608579 and in part by the Alexander von Humboldt Foundation through Dr. Ian Akyildiz's Humboldt Research Prize in Germany. An earlier version of this paper appeared in the IEEE International Conference on Communications, Sydney, NSW, Australia, June 10–14, 2014 [1]. Associate Editor: E. Grossman.

C. Han is with the University of Michigan–Shanghai Jiao Tong University Joint Institute, Shanghai Jiao Tong University, Shanghai 200240, China (e-mail: chong.han@sjtu.edu.cn).

Ian F. Akyildiz is with the Broadband Wireless Networking Laboratory, School of Electrical and Computer Engineering, Georgia Institute of Technology, Atlanta, GA 30332 USA (e-mail: ian@ece.gatech.edu).

Color versions of one or more of the figures in this paper are available online at http://ieeexplore.ieee.org.

Digital Object Identifier 10.1109/TTHZ.2016.2569460

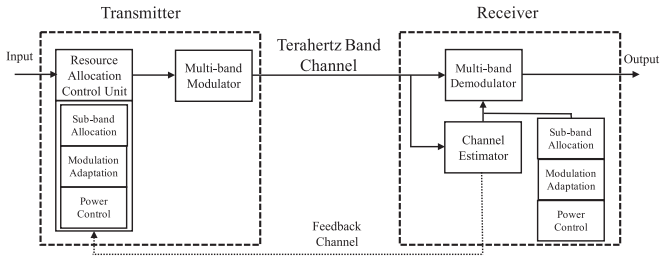

Fig. 1. System model of the distance-aware BW-adaptive resource allocation scheme, by using the control unit.

In this paper, we develop a distance-aware BW-adaptive resource allocation scheme for THz band communication networks with the objective to improve the distance. The developed scheme captures the unique channel peculiarities including the relationship between the distance and the BW, and strategically utilizes the spectrum to enable multiple ultrahigh-speed links in long-range networks. In particular, this scheme determines the BW as a function of the distance, and has three functionalities: subwindow allocation, modulation adaptation, and transmit power controlling. These interrelated functionalities of resource allocation are realized in the control unit. A system model that employs this resource allocation scheme is illustrated in Fig. 1.

The main contributions of this paper are summarized as follows.

1) *We develop a distance-aware BW-adaptive resource allocation scheme in the THz band communication network*, which captures the peculiarities of distance-varying spectral windows and efficiently exploits the Terahertz spectrum. The solutions to the BW utilization, the spectrum allocation, the modulation techniques, and the transmit power are jointly derived, aiming to improve the communication distance and concurrently support multiple ultrahigh-speed links.
2) *We propose a strategic spectrum allocation principle* for the multiuser network to intelligently allocate the center spectrum of the spectral windows to the long-distance users first, and then the side spectrum to the short-distance users. Theoretical bounds on the network data rate are analyzed.

In the formulated optimization frameworks for the single-user and multiuser cases, the objective focuses on the distance maximization, and the constraints cover the transmit power, the BW, the error rate, and the data rate, which are all closely related to the physical parameters such as the path loss, the delay, and the coherence BW that result from the unique THz channel. Then, an optimal solution based on the KKT method is analytically derived for the single-user case, while a suboptimal solution based on our proposed strategic spectrum allocation principle is provided for the multiuser case. Numerical results show that the developed schemes can effectively improve the spectrum utilization and enable multiple ultrahigh-speed links in the THz band networks.

The remainder of this paper is organized as follows. In Section II, channel characteristics in the THz band are analyzed. The resource allocation for the single-user communication is formulated and an optimal solution is derived in Section III. Then, we propose the strategic spectrum allocation principle, and develop the resource allocation scheme in the multiuser network in Section IV. The extensive numerical analysis for both single-user and multiuser cases is provided in Section V. Finally, the paper is concluded in Section VI.

II. Terahertz Band Channel Characterization

In this section, we provide an overview of the THz band channel and its associated characteristics. In particular, the distance-varying spectral windows, the delay spread, and the coherence BW are investigated for the THz frequencies. Based on these characteristics, we highlight the design implications for the THz band communication.

A. Overview of the Terahertz Band Channel

Due to the frequency dependence appearing in the propagation channel and antennas, a multipath (MP) propagation model in the THz band is developed as the combination of many individual subwindows in our previous work [7]. The line-of-sight (LOS) and the reflected rays are included in this MP model, while scattered and diffracted rays are neglected since they have insignificant contributions to the received signal power. We denote t as the time and d as the communication distance. By including $N_{\mathrm{Ref}}^{(u)}$ reflected rays, the channel response of the MP model in the uth frequency subwindow is given by

$$h_u(d) = \alpha_{\mathrm{LOS}}^{(u)}(d)\delta(t - t_{\mathrm{LOS}})\mathbb{1}_{\mathrm{LOS}} + \sum_{q=1}^{N_{\mathrm{Ref}}^{(u)}} \alpha_{\mathrm{Ref}}^{(u,q)}(d)\delta(t - t_{\mathrm{Ref}}^{(q)}) \quad (1)$$

where $\mathbb{1}_{\mathrm{LOS}}$ is the indicator function that is equal to 1 or 0 for the presence of LOS path or not. For the LOS path, $\alpha_{\mathrm{LOS}}^{(i)}$ refers to the attenuation, and t_{LOS} stands for the delay. For the $q\mathrm{th}$ reflected path, $\alpha_{\mathrm{Ref}}^{(i,q)}$ is the attenuation and $t_{\mathrm{Ref}}^{(q)}$ is the delay. In the $u\mathrm{th}$ frequency subwindow, the center frequency is denoted by f_u. The total number of MP components is given by $N_u = \mathbb{1}_{\mathrm{LOS}} + N_{\mathrm{Ref}}^{(u)}$, with $N_{\mathrm{Ref}}^{(u)} < 10$ [5]. On the one hand, the MP signal consists of the LOS and multiple reflected paths, when the gains of the transmitting and receiving antennas are $G_t = G_r = 0$ dBi. On the other hand, with the use of high-gain antennas or very large antenna arrays, the number of MP rays and the delay spread decrease, while the total received signal power increases. In particular, when the gains of the transmitting and receiving antennas are $G_t = G_r = 20$ dBi, the THz band transmission is highly directional and the number of MP components reduces to a small number, i.e, $N_u = 1$.

B. Distance-Varying Spectral Windows

To analytically characterize the distance-varying spectral windows, we define the path loss threshold $\mathrm{PL}_{\mathrm{th}}$. The spectrum that has smaller path loss than this threshold forms the spectral windows. This path loss threshold is computed by invoking the

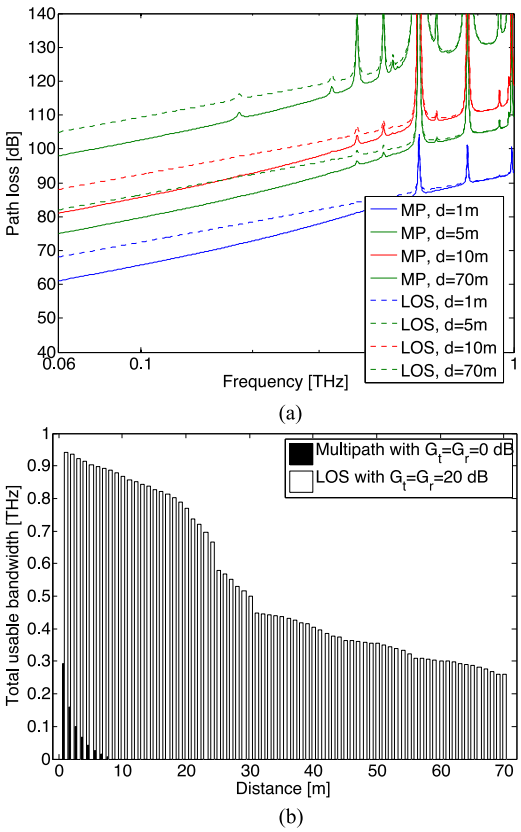

Fig. 2. Channel characterization of the THz band for MP and directional transmission through LOS. (a) Distance-varying path loss. (b) Total usable BW.

link budget equation as

$$PL_{\rm th} = P_{\rm Tx} + G_t + G_r - \gamma_{\rm th} - P_w \tag{2}$$

where $P_{\rm Tx} = 10$ dBm refers to the transmit power, and $\gamma_{\rm th} = 10$ dB stands for the threshold SINR. We note that the ambient noise in the THz band channel is mainly contributed by the molecular absorption noise, which is frequency-dependent and colored, as suggested in [18]. Besides the ambient noise originated in the channel, a major noise source comes from the receiver, which depends on the device technology in use. As adopted in [14] and [19], we consider that the noise effect can be approximated as a white Gaussian noise, with the power $P_w = -80$ dBm. Using this threshold, we determine the spectral windows and the total usable BW for the different transmission cases.

1) Spectral Windows for $G_t = G_r = 0$ dBi: In the MP propagation model, we consider the received signal as a constructive superposition of the LOS and four reflected paths, over the frequency band 0.06 to 1 THz, where the material parameters are readily available [7]. The path loss values for the different distances are shown in Fig. 2(a), where the threshold is 80 dB. In this case, the communication distance is limited up to 8 m for the MP propagation. At the distance above 8 m, there is no usable spectrum in the THz band. Below 8 m, the total usable BW is illustrated in Fig. 2(b), which is equal to 0.29 THz at $d = 1$m. The decreasing rate from $d = 1$ to 8 m is 40.91 GHz/m.

2) Spectral Windows for $G_t = G_r = 20$ dBi: With the use of the high antenna gains, the transmission is directional through the LOS path in one narrow beam. The path loss of the LOS consists of the spreading loss and the molecular absorption loss [18], and is shown in Fig. 2(a). According to (2), the path loss threshold is enhanced to 120 dB. The path loss peaks caused by the molecular absorption create spectral windows, which have different BW, and drastically change with the variation of the distance. A few path loss peaks appear over this frequency band, such as at 0.56, 0.75, and 0.98 THz, and the number of peaks increases with the distance. According to this threshold value, the total BW over the THz spectrum is identified in Fig. 2(b), for the different distances. For example, the total BW over the 0.06–1 THz band shrinks from 0.94, 0.87, 0.50 to 0.26 THz, when the distance rises from 1, 10, 30 to 70 m. The decreasing rate of the total usable BW from 1 to 70 m this range is small and equals to 9.9 GHz/m.

C. Delay Spread

In the MP channel, the delay spread is a measure of how dispersive the channel is, which reduces as the antenna directivity increases. This temporal parameter relates to the performance degradation caused by ISI and useful for the physical system design. Moreover, the coherence BW, that is defined as the range of frequencies over which channel correlation exceeds 50%, is given by $0.2/\sigma_u$ where σ_u refers to the rms delay spread of the MP channel. For example, at $f = 0.3$ THz and $d = 5$ m, the coherence BW for the MP propagation is 1 GHz, over which the channel experiences flat fading. Due to the decrease of the beam width in the directional antenna (DA) case, the number of significant MP components decreases. Hence, the rms delay spread reduces and the coherence BW rises.

D. Design Guidelines

The very strong relationship between the distance, the spectral windows, and the total usable BW in Fig. 2(b) motivates the development of *distance-aware BW-adaptive* transmission schemes. Moreover, the ultrabroad BW of the spectral window ranges from multi-GHz to THz, which allows the multiband transmission by dividing each spectral window into many subwindows. The utilization of the subwindows needs to be intelligently selected to avoid spectrum with the path loss peaks. For example, in the MP propagation with $d = 5$ m, the spectrum above 0.1 THz has significantly large path loss and cannot be used. In the directional propagation, the communication around 0.56, 0.75, and 0.98 THz need to be prevented.

As a result, the created subwindow has smaller BW and supports slower data rates, which effectively relaxes the design requirements of individual subwindows, and is helpful for THz band communication to process very high data rates. Over each band, adaptive modulation can be used for transmission for the features of spectral efficiency and in conjunction with the design of transmit power and error rate. These resource allocation techniques have been well explored for lower frequencies in [8]–[10], [20]. In the realm of THz band communications, the distance improvement becomes the focus, and moreover, the

available BW varies over the different distances. Furthermore, the peculiarities of the channel lead us to rethink the physical parameters in the resource allocation scheme, as follows. From the investigation in Section II-C, the width of the subwidth can be set as $B_g = 1$ GHz, which is smaller than the coherence BW. This eliminates the ISI effects and thereby, allows the narrowband communication over each subwindow. However, in this multiband system, the interband interference (IBI) occurs which causes from the power leakage from the neighboring subwindows. Hence, the subwindow width (B_g), the utilization and the allocation of the spectrum, the IBI, the transmit power, and the modulation schemes, and the distance enhancement, need to be thoroughly investigated in the THz band communication network.

For each subband or subwindow, we consider that a single carrier is implemented in an individual modulator/demodulator circuit at the transmitter/receiver. The overall multiband modulators/demodulators are included in the system design in Fig. 1. Then, the signal over each subband is radiated by using an individual THz antenna with a directivity gain. Thanks to the very small wavelengths at THz frequencies, the multiband architecture can be implemented by using the graphene-based nanoantenna [21], [22] and nanotransceiver [23], [24] technologies, among others. Although orthogonal frequency-division multiplexing (OFDM) is suggested for 60 GHz systems to enhance the spectral efficiency [25], the BW is not scarce in the THz band. Furthermore, the very complex transceivers, high peak-to-average power ratio, and strict requirements for frequency synchronization make OFDM very challenging in the THz band, where digital processors that can handle such very high data rates (e.g., over 1 Tb/s) do not exist to date. On the contrary, the multiband system allows nonoverlapping utilization of the spectrum to improve the spectrum efficiency compared to the pulse-based systems [13], [14], while has less complex transceivers and more relaxed synchronization requirements than OFDM systems.

III. Distance-Aware BW-Adaptive Resource Allocation: Single User

In this section, we develop the distance-aware BW-adaptive resource allocation scheme in the single-user communication. The objective is to increase the communication range and explore the relationship between the distance and the BW. This can be realized by maximizing the data rate, since it decreases monotonically as the distance rises. In this case, the available spectrum is determined as a function of the link distance and the entire BW is allocated to one user. Then, once the data rate requirement is determined, the largest attainable distance is obtained accordingly.

A. Signal-to-Interference-Plus-Noise Ratio (SINR)

For a communication distance d, we consider that there are $U(d)$ subwindows or subbands for transmission. We first determine the expression for the SINR, which is affected by the transmit power, the channel gain, the interference, and the noise. In particular, the interference associated with the multiband system includes the ISI and the IBI. ISI is negligible in the narrowband communication over each subwindow. The IBI captures the power leakage from the surrounding subwindows, and increases if the separation between the consecutive subwindows (i.e., the BW of the subwindow) decreases. With the use of high-gain antennas, the delay spread reduces significantly and the channel frequency response varies less frequency selective. However, the path loss of the channel is reduced and, hence, the IBI becomes more significant in this case.

In the THz band, the number of subwindows is at the order of multiple tens. To model this interference, we invoke the central limit theorem to approximate the IBI with a Gaussian process. The IBI accounts for the power leakage from the surrounding subwindows. It is shown in [14] and [26] that the interference from the adjacent frequency bands can be approximated as a Gaussian distributed random variable. The distribution of the interference power on the uth subwindow that superimposes from the other subwindows follows:

$$I_B^u \sim \mathcal{N}\left(0, \int_{f_u} \sum_{v,v\neq u}^{U(d)} P_v |G^v(f_u)| \sum_{m=1}^{N_u} \boldsymbol{\alpha}^{(v)}(m)|^2 df_u\right) \quad (3)$$

where G^v describes the waveform. The interference on the uth subwindow is contributed as the power leakage from the vth subwindow with $v \neq u$. Moreover, from the channel model in (1), the path attenuation

$$\boldsymbol{\alpha}^{(v)} = \left[\alpha_{\mathrm{LOS}}^{(v)}, \alpha_{\mathrm{Ref}}^{(v,1)}, \ldots, \alpha_{\mathrm{Ref}}^{(v,N_{\mathrm{Ref}}^{(v)})}\right].$$

Next, the instantaneous SINR in the uth subwindow, $\gamma_u(d)$, is analyzed, which is affected by the channel response, the transmit power, the interference, and the noise, as

$$\gamma_u(d) = \frac{G_t G_r |h_u(d)|^2 P_{\mathrm{Tx}}}{G_t G_r I_B^u + B_g S_w} \quad (4)$$

where h_u is the channel response in the uth subwindow given in (1), P_{Tx} represents transmit power in (2), S_w denotes the noise power spectral density, and I_B^u is the interference from (3). As a function of the instantaneous SINR in (4), the received SINR in this subwindow equals to $\gamma_u\ (P_u(\gamma)/P_{\mathrm{Tx}})$, with P_u standing for the transmit power that is allocated on the uth subwindow.

B. Resource Allocation Model

In the single-user communication, the broad BW in the THz band enables very high data rate transmission. Hence, different from the traditional resource allocation problem which either minimizes the energy consumption or maximizes the data rate, distance maximization becomes the objective, while the data rate needs to exceed some threshold.

In order to address this distance maximization problem efficiently, we transform it into a set of data rate maximization problems for different distances. Then, the solution to the original distance maximization problem is found at d^*, when the transformed optimal data rate drops to the threshold $R_{\mathrm{su}}^{\mathrm{th}}$ at the distance d^*. Since the resource allocation problem for data rate maximization is well investigated and the optimal solution requires low complexity, the distance maximization in the realm

of the THz band communication can be solved efficiently. To start with, the original distance maximization problem is written as

$$\text{Objective:} \quad \max \quad d \tag{5}$$

$$\text{Subject to:} \quad R_{\text{su}}(d) > R_{\text{su}}^{\text{th}}. \tag{6}$$

To transform this into the data rate maximization, we first express the single-user data rate at one particular distance as the sum of the data rates on individual subwindows as

$$\text{Transformed objective:} \quad \max_{P_u, k_u} R_{\text{su}}(d) = B_g \sum_{u=1}^{U(d)} k_u(\gamma_u(d)). \tag{7}$$

The solution to the distance maximization problem is found by iteratively solving (7) with the increasing d to satisfy (6).

Note that the SINR is a function of the distance and the transmit power P_u depends on the SINR. For conciseness, these dependencies are declared when the parameters are defined, whereas the dependencies are omitted in the later equations. Moreover, ϵ_u refers to the bit error rate (BER) on the $u\text{th}$ subwindow, which is a function of the SINR as well. In particular, the BER expression of square MQAM as a function of SINR is approximated as [12]

$$\epsilon_u(\gamma_u(d)) \approx 0.2 \exp\left(\frac{-1.5\gamma_u\left(P_u/P_{\text{Tx}}\right)}{2^{k_u}-1}\right). \tag{8}$$

For a given BER, the rate on the subwindow in (7) is obtained by rearranging (8)

$$k_u(\gamma_u(d)) = \log_2\left(1 - \frac{1.5\gamma_u\left(P_u/P_{\text{Tx}}\right)}{\ln\left(5\epsilon_u\right)}\right) \tag{9}$$

where the expression in $\log(\cdot)$ represents the maximum constellation of MQAM that can be supported, as a function of the BER, the transmit power, and the SINR.

There are two constraints associated with the single-user optimization problem. First, the total transmit power for each user is bounded by

$$\text{Constraint 1:} \quad \sum_{u=1}^{U(d)} P_u(\gamma_u(d)) \le P_{\text{Tx}} \tag{10}$$

where P_{Tx} is the threshold of the transmit power budget. The second constraint is for the error rate, which is equivalent to the constraint on the SINR per bit in the communication system. Specifically, the average BER $\bar{\epsilon}$ as

$$\text{Constraint 2:} \quad \bar{\epsilon} = \frac{B_g \sum_{u=1}^{U(d)} \epsilon_u \cdot k_u}{B_g \sum_{u=1}^{U(d)} k_u} \le \epsilon_{\text{th}} \tag{11}$$

where ϵ_{th} refers to the average BER threshold value, and the BER is derived in (8), which is related to the SINR, the distance, the modulation scheme, and the transmit power.

C. Solution

This constrained optimization problem with inequalities can be solved by using the KKT method [27], [28], with the convex objective of maximizing the data rate. By defining the KKT multipliers $\mu_1, \mu_2 \ge 0$, we obtain the Lagrangian function as

$$\begin{aligned} L(P_u, k_u, \mu_1, \mu_2) = & \sum_{u=1}^{U(d)} k_u + \mu_1 \left[P_{\text{Tx}} - \sum_{u=1}^{U(d)} P_u\right] \\ & + \mu_2 \left[\epsilon_{\text{th}} B_g \sum_{u=1}^{U(d)} k_u - B_g \sum_{u=1}^{U(d)} \epsilon_u \cdot k_u\right]. \end{aligned} \tag{12}$$

By differentiating the Lagrangian function with respect to the power adaptation and transmutation rate, we can obtain the KKT necessary conditions for the optimal solutions, as

$$\frac{\partial L}{\partial P_u} = 0 \tag{13}$$

$$\frac{\partial L}{\partial k_u} = 0. \tag{14}$$

The above condition (13) can be rearranged since k_u is not a function of P_u, as

$$-\mu_1 - \mu_2 \cdot B_g k_u \frac{\partial \epsilon_u}{\partial P_u} = 0. \tag{15}$$

By recalling (8), the derivative of the error probability can be rearranged as

$$\begin{aligned} \frac{\partial \epsilon_u}{\partial P_u} &= \frac{\partial\left[0.2 \exp\left(\frac{-1.5\gamma_u\left(P_u/P_{\text{Tx}}\right)}{2^{k_u}-1}\right)\right]}{\partial P_u} \\ &= -\frac{1.5\gamma_u/P_{\text{Tx}}}{2^{k_u}-1} \cdot \epsilon_u. \end{aligned} \tag{16}$$

By combining (15) and (16), the BER adaptation is obtained as

$$\epsilon_u = \frac{P_{\text{Tx}}\mu_1}{\mu_2 B_g k_u} \cdot \frac{2^{k_u}-1}{1.5\gamma_u}. \tag{17}$$

This can be interpreted that the error probability decreases as the channel quality [i.e., the SINR in (17)] increases, which is matching with the water-filling principle. From (14), we obtain

$$1 + \mu_2 \epsilon_{\text{th}} B_g - \mu_2 \frac{\partial \epsilon_u}{\partial k_u} \cdot B_g k_u - \mu_2 \epsilon_u B_g = 0. \tag{18}$$

By recalling (8), the derivative of the error probability can be rearranged as

$$\frac{\partial \epsilon_u}{\partial k_u} = \epsilon_u \cdot \frac{1.5\gamma_u\left(P_u/P_{\text{Tx}}\right)}{\left(2^{k_u}-1\right)^2} \cdot 2^{k_u} \ln(2). \tag{19}$$

Then, to combine (17), (18), and (19), the power adaptation that maximizes the data rate is

$$\begin{aligned} \frac{P_u}{P_{\text{Tx}}} &= \max\left\{\left[\frac{1+\mu_2\epsilon_{\text{th}}B_g}{\mu_2\epsilon_u B_g} - 1\right] \cdot \frac{\left(2^{k_u}-1\right)^2}{1.04 \cdot \gamma_u 2^{k_u} k_u}, 0\right\} \\ &= \max\left\{\frac{\left(2^{k_u}-1\right)\left(1+\mu_2\epsilon_{\text{th}}B_g\right)U(d)}{P_{\text{Tx}}\mu_1 2^{k_u}\ln(2)}\right. \\ &\qquad \left. - \frac{\left(2^{k_u}-1\right)^2}{1.04 \cdot \gamma_u 2^{k_u} k_u}, 0\right\}. \end{aligned} \tag{20}$$

Algorithm 1: Resource allocation in single-user THz band communication.

Initialization: choose two constants μ_1, μ_2, and set $P_u = \epsilon_u = 0$
while $\sum_{u=1}^{U(d)} [P_u] \leq P_{\mathrm{Tx}}$ and $\overline{\epsilon} \leq \epsilon_{\mathrm{th}}$ **do**
  Step 1: Define SINR boundaries, $\hat{\gamma}_i \leftarrow \mu_1 \cdot \frac{2^{\hat{k}_m}-1}{\hat{k}_m}$, $m = 1, 2, 3, 4, 5, 6$
  if $k_u > 0$ **then**
    Step 2: Determine rate, k_u, using (23) and the defined SINR boundaries for each γ_u
    Step 3: Calculate BER, $\epsilon_u \leftarrow \frac{P_{\mathrm{Tx}}\mu_1}{\mu_2 B_g k_u} \cdot \frac{2^{k_u}-1}{1.5\gamma_u}$
    Step 4: Find power allocation, $P_u \leftarrow -P_{\mathrm{Tx}} \ln(5\epsilon_u) \frac{2^{k_u}-1}{1.5\gamma_u}$
  end if
  Decrease μ_1 and increase μ_2
end while

By including (4), the solution to the power adaptation is

$$\frac{P_u}{P_{\mathrm{Tx}}} = \max\left\{ \frac{\left(2^{k_u}-1\right)\left(1+\mu_2\epsilon_{\mathrm{th}}B_g\right)}{P_{\mathrm{Tx}}\mu_1 2^{k_u}\ln(2)} - \frac{\left(2^{k_u}-1\right)^2\left(G_tG_rI_B^u + B_gS_w\right)}{1.04\cdot G_tG_r|h_u(d)|^2 P_{\mathrm{Tx}}2^{k_u}k_u}, 0 \right\}. \quad (21)$$

The constellation adaptation k_u that is defined in (9) is either zero or the nonnegative solution of the following equation, by recalling (9), (17), and (21):

$$\frac{1+\mu_2\epsilon_{\mathrm{th}}B_g}{P_{\mathrm{Tx}}\mu_1 2^{k_u}\ln(2)} - \frac{(2^{k_u}-1)(G_tG_rI_B^u + B_gS_w)}{1.04G_tG_r|h_u(d)|^2 P_{\mathrm{Tx}}2^{k_u}k_u} = -\frac{1}{1.5\gamma_u}\ln\left(\frac{P_{\mathrm{Tx}}\mu_1}{\mu_2 B_g k_u}\cdot\frac{(2^{k_u}-1)(I_B^u + B_gS_w)}{0.3G_tG_r|h_u(d)|^2 P_{\mathrm{Tx}}}\right). \quad (22)$$

The values of the modulation rate k_u and the KKT multipliers μ_1 and μ_2 can be found through a numerical search, to satisfy the transmit power and the BER constraints.

In practice, the transmission rate is discrete and varied within a fixed set [12]. For example, if we select no transmission, BPSK, 4-QAM, 16-QAM, 64-QAM, 256-QAM, and 1024-QAM as the MQAM candidates, the rate $k_{u,v}$ takes the value in the set $\{0, 1, 2, 4, 6, 8, 10\}$ b/symbol. Correspondingly, there are six boundary SINR values, namely $\{\hat{\gamma}_m, m = 1, 2, 3, 4, 5, 6\}$, which are used to assign the transmission rate $\{\hat{k}_m\}$. In particular, the rate on each subwindow is determined by using the following piecewise function:

$$k_u = \begin{cases} 0, & \text{if } \gamma_u < \hat{\gamma}_1 \\ 1, & \text{if } \hat{\gamma}_1 \leq \gamma_u < \hat{\gamma}_2 \\ \vdots & \vdots \\ 10, & \text{if } \hat{\gamma}_6 \leq \gamma_u. \end{cases} \quad (23)$$

As a result, the rate adaptation corresponds to finding the rate region boundaries. If we further assume that the power adaption P_u is continuous at each boundary [12], we obtain the solutions to the optimization framework by using Algorithm 1. To start with, we define two constants μ_1 and μ_2, which will be updated at each iteration. First, the SINR boundaries are defined. They are used to determine the transmission rate on each subwindow at the second step. Then, the BER and transmit power allocation are computed at the third and fourth steps. To finish, we decrease μ_1 and increase μ_2. In the next iteration, we check the current transmit power and the average BER. If both of these constraints are satisfied, we proceed to the first step and repeat the process. Otherwise, we acquire the desired values for P_u, k_u and the iteration is completed.

By using the aforementioned algorithm, the analytical solution to maximize the rate for a distance in (7) can be acquired efficiently. Then, the solution to the original distance maximization problem in (5) is found at d^*, when the optimal data rate $R_{\mathrm{su}}(d^*)$ drops to $R_{\mathrm{su}}^{\mathrm{th}}$ as in (6). Since the resource allocation problem for the data rate maximization has analytical solution with a low complexity, the original resource allocation problem for the distance maximization in the THz band can be solved efficiently.

IV. Distance-Aware BW-Adaptive Resource Allocation: MultiUser

In the single-user case, the communication range and the data rate are maximized by intelligently adapting the transmit power and the modulation technique on each subwindow. For example, the data rate over 100 Gb/s (as studied in [1] and in Section V-A) is attainable for distance up to 21 m, by applying the distance-aware BW-adaptive resource allocation scheme in the directional transmission. However, the actual utilized BW to enable this ultrahigh-speed link is 0.06–0.12 THz or equivalently, 60 subwindows. Being motivated by this spectrum underexploitation, our aim is to seek for the bound on how many ultrahigh-speed links can be simultaneously supported in the THz band. To achieve this goal, in this section, we propose a novel strategic spectrum allocation principle adjunct with the distance-aware BW-adaptive resource allocation scheme in the multiuser case.

A. Strategic Spectrum Allocation

In a multiuser network, there are I transmission links to be allocated. We sort the links in a descending order according to the distance, such as $d_1 > \cdots > d_i > \cdots > d_I$. Without loss of generality, we analyze one spectral window in the THz band in Fig. 3(a). As the distance decreases, the path loss drops, and hence, the received power (P_R) and the usable BW of this window increase, for example, from d_1 to d_2 and d_3. Based on this relationship, the strategic spectrum utilization principle is presented in Fig. 3(b), and summarized as follows. First, the center subwindows, i.e., the center spectrum in the window, are allocated to the long-distance links. Then, the side subwindows, i.e., the side spectrum in the window, are allocated to the short-distance transmissions.

Based on this principle, on the one hand, the information on the side subwindows cannot reach the long-distance users due to the very high path loss. On the other hand, the information on the central subwindows can reach not only the intended

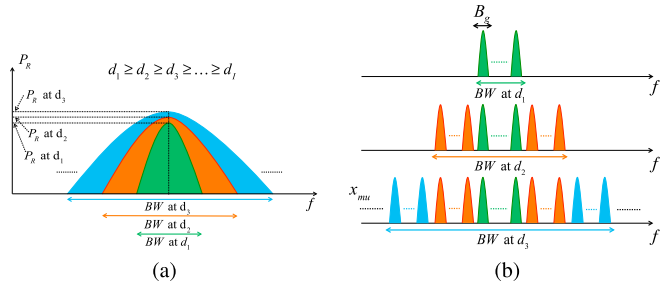

Fig. 3. Multiuser communication network. (a) Receive power and BW. (b) Illustration of the proposed spectrum allocation principle.

long-distance users, but also the unintended short-distance users, which causes interference. However, this interference to the short-distance users can be effectively mitigated in the multicarrier communication scheme [29]. As a consequence, this strategic principle efficiently utilizes the spectrum and benefits from the unique relationship between the BW and the distance in the THz band. Note that the distance difference between the consecutive links, for example, $d_i - d_{i+1}$, needs to be sufficiently large, so that there is enough BW to be further exploited to support $R^{i+1}_{\rm mu}(d_{i+1}) \geq R^{\rm th}_{\rm mu}$, where $R^{\rm mu}_{\rm th}$ represents the data rate threshold in the multiuser network.

B. Resource Allocation Model

By incorporating this spectrum allocation principle, we formulate the resource allocation model. In a THz band communication network, there is an existing link over the distance d_1. The data rate of this link satisfies the requirement of the ultrahigh-speed transmission, $R^{\rm th}_{\rm mu}$, i.e., $R^1_{\rm mu}(d_1) \geq R^{\rm th}_{\rm mu}$. On the one hand, we focus on addressing the distance challenge in the THz band communication. On the other hand, the resource allocation model in the multiuser network needs to support multiple ultrahigh-speed links at the same time. Therefore, the objective of our strategic spectrum allocation principle is to maximize the total distance $\sum_{i=1}^{I} d_i$, where I represents the number of transmission links reaching the ultrahigh-speed threshold. Then, the data rate becomes a constraint that needs to exceed a threshold (i.e., 10 or 100 Gb/s), thanks to the very broad BW in the THz band.

The variables associated in this scheme include the transmit power, the modulation scheme, and the subwindow allocation. We describe the resource allocation model as

$$\max_{P^i_u, k^i_u, \rho^i_u} \quad \sum_{i=1}^{I} d_i \tag{24}$$

$$\text{subject to} \quad \sum_{u=1}^{U(d)} P^i_u \cdot \rho^i_u \leq P_{\rm Tx}, \ \text{for all } i \in \{1, \ldots, I\} \tag{25}$$

$$\frac{B_g \sum_{u=1}^{U(d)} \epsilon^i_u k^i_u \rho^i_u}{B_g \sum_{u=1}^{U(d)} k^i_u \rho^i_u} \leq \epsilon_{\rm th}, \quad \text{for all } i \in \{1, \ldots, I\} \tag{26}$$

$$\sum_{i=1}^{I} \rho^i_u = 1, \quad \text{for all } u \in \{1, \ldots, U\} \tag{27}$$

$$R^i_{\rm mu}(d_i) \geq R^{\rm th}_{\rm mu}, \quad \text{for all } i \in \{1, \ldots, I\}. \tag{28}$$

In (25), the transmit power on each individual subwindow P^i_u needs to satisfy that the total transmit power for each user is bounded by $P_{\rm Tx}$. The average BER for each user's transmission needs to satisfy the constraint in (26), in which $\epsilon^i_u(\gamma)$ refers to the BER of the ith user in the uth subwindow. Moreover, we define the sharing factor ρ, which is dependent on the transmission rate, as

$$\rho^i_u = \begin{cases} 1, & \text{if } \ k^i_u > 0 \\ 0, & \text{if } \ k^i_u = 0. \end{cases} \tag{29}$$

The constraint in (27) implies that one subwindow is occupied by at most one user. Finally, the data rate on each link needs to exceed the threshold value for ultrahigh-speed communication, as expressed in (28). The calculation of this data rate is described as

$$R^i_{\rm mu}(d_i) = B_g \sum_{u=1}^{U(d)} k^i_u \cdot \rho^i_u \tag{30}$$

where d_i denotes the distance of the ith link. These link distances in the multiuser case are randomly generated by following the Uniform distribution, as

$$d_i \sim U[d_{\min}, d_{\max}] \tag{31}$$

where $d_{\min}$ is the lower-bound distance, and $d_{\max}$ refers to the upper-bound distance. In the multiuser case, the SINR for the ith user on the uth subwindow $\gamma^i_u(d_i)$ is defined as

$$\gamma^i_u(d_i) = \frac{G_t G_r |h_u(d_i)|^2 P_{\rm Tx}}{G_t G_r I^u_B + B_g S_w} \tag{32}$$

where the IBI is taken into account as given in (3) which includes the effect of the multiuser interference. The SINR determines the allocation of the transmit power, the rate, and the subwindow utilization. In particular, if the SINR is below than the threshold $\hat{\gamma}_1$ in (23), no transmit power is allocated since no transmission occurs, which equivalently to suggest that S^i_u, k^i_u, ρ^i_u are all zeros in this subwindow.

C. Solution

In the multiuser resource allocation problem, there are totally 3I+U constraints and 3UI variables. To avoid the high complexity of solving this problem, we propose a suboptimal solution, which efficiently allocates the transmit power, the modulation scheme, and the subwindow. Numerical results in Section V will show that the proposed solution with the strategic spectrum allocation (in Section IV-A) can achieve better results than the existing solutions.

The flowchart to search for the solutions to (24) is demonstrated in Fig. 4, and is explained as follows. First, we sort the links in the network by distances. We initialize the flow by defining a spectrum/subwindow pool $\overrightarrow{SP}$, which contains the

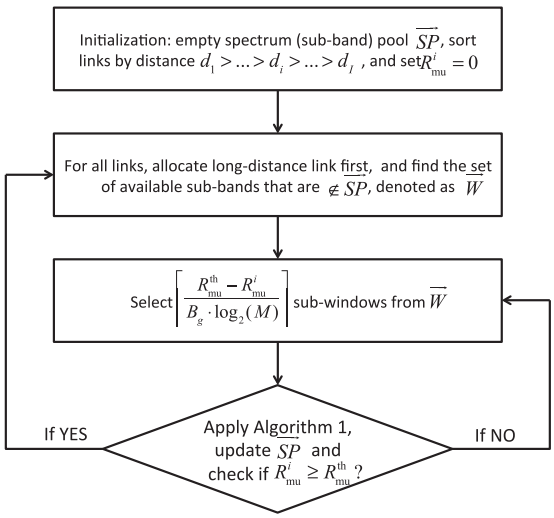

Fig. 4. Flowchart for the distance-aware BW-adaptive resource allocation in multiuser networks.

set of subwindows that have already been occupied. Second, starting with long-range communication, we identify the set of available subwindows $\overrightarrow{W}(d_i)$, which are determined based on the transmission distance and are not contained in the spectrum pool, i.e., $w \notin \overrightarrow{SP}$ for all $w \in \overrightarrow{W}(d_i)$. Third, we estimate the number of additional subwindows that is needed for the current user to satisfy $R_i \geq R_{\mathrm{th}}$, which is calculated as

$$\text{Number of subwindows} \geq \left\lceil \frac{R^{\mathrm{th}}_{\mathrm{mu}} - R^i_{\mathrm{mu}}}{B_g \log_2(M)} \right\rceil \tag{33}$$

where $\lceil \cdot \rceil$ stands for the ceiling function. This can be explained that the number of subwindows is at least equal to the ratio of the total demanding data rate and the largest rate per subwindow. Here, M represents the M-QAM modulation and we obtain the number of subwindows by choosing $\log_2(M) = 10$ for 1024-QAM, which is the lower bound of the subwindows that are needed, as considered in Section III. Fourth, after completing the subwindow allocation, we perform Algorithm 1 to compute the data rate, and update the spectrum pool based on the sharing factor information as defined in (27). Finally, we check whether the current data rate satisfies the threshold as defined in (28). If the rate constraint is satisfied, we proceed to repeat the procedures for the next-farthest link. Otherwise, we allocate more subwindows to the current link by using the updated data rate and spectrum pool information.

After iterating these steps until all the links are completed, the solutions to the allocated transmit power, the modulation over each subwindow, and the distribution of the subwindows are obtained. However, if the spectrum resources are fully assigned, i.e., there is no w such that $w \notin \overrightarrow{SP}$ and $w \in \overrightarrow{W}(d_i)$, I links cannot be accommodated simultaneously for ultrahigh-speed transmissions in the THz band. Hence, the network data rate $R^{\mathrm{Tot}}_{\mathrm{mu}}$ is equal to the sum of data rates for individual links

$$R^{\mathrm{Tot}}_{\mathrm{mu}} = \sum_{i=1}^{I} B_g \sum_{u=1}^{U(d)} k^i_u \cdot \rho^i_u. \tag{34}$$

D. Discussions

The objective of our strategic spectrum allocation principle is to maximize the total distance $\sum_{i=1}^{I} d_i$ in (24), since the distance limitation poses the main challenge for THz band communication networks. This is different from the multiuser resource allocation schemes for the lower microwave frequencies, in which the data rate or the power consumption is the challenge. For the microwave frequencies, the objective in the resource allocation schemes is either maximizing the total data rate or minimizing the total power consumption [11].

In our analysis, a static user topology in the THz band communication network is considered, based on a centralized architecture with the use of an access point (AP) [4]. The AP performs the proposed BW-adaptive resource allocation scheme to strategically allocate the spectrum. If a new user requests an admission to the network, the AP could allocate the remaining available subwindows by referring to the spectrum pool and decide the communication parameters, as suggested in Fig. 4. Moreover, the constraints in (25)–(28) need to be satisfied for a successful user admission, while the objective in (24) might become invalid. However, it is possible that the remaining subwindows in the THz band are insufficient to support the new user for the ultrahigh-speed communication. On the other hand, to solve for the objective in (24), the AP needs to reperform the resource allocation scheme for all the users (i.e., including the new user), as described in Section IV-C.

In the formulated optimization frameworks for the single-user (see Section III) and multiuser (see Section IV) cases, the objective focuses on the distance maximization, and the constraints cover the transmit power, the BW, the error rate, and the data rate, which are all closely related to the physical parameters such as the path loss, the delay, and the coherence BW that result from the unique THz band channel as analyzed. Then, an optimal solution based on the KKT method is analytically derived for the single-user case, while a suboptimal solution based on our proposed strategic spectrum allocation principle is provided for the multiuser case.

V. Performance Evaluation

In this section, we numerically evaluate the performance of the distance-aware BW-adaptive resource allocation scheme in both single-user and multiple-user regimes. The developed model is unified in the (0.06–10) THz band, while the performance evaluations are limited up to 1 THz where the parameters of material properties are readily available [7].

The discrete MQAM signal constellation chooses from no transmission, BPSK, 4-QAM, 16-QAM, 64-QAM, 256-QAM, and 1024-QAM, which corresponds to the modulation rate $k^i_u \in \{0, 1, 2, 4, 6, 8, 10\}$ b/Hz as in Section III-C. We consider the BER requirement in (11) as $\epsilon_{\mathrm{th}} = 10^{-3}$. For performance comparison, we apply our resource allocation scheme on the state-of-the-art millimeter wave systems at 0.3 [30] and 0.06 THz [31]. In particular, the transmission at 0.3 THz occupies the fixed 50 GHz BW, while the transmission at 60 GHz uses the fixed 10 GHz BW.

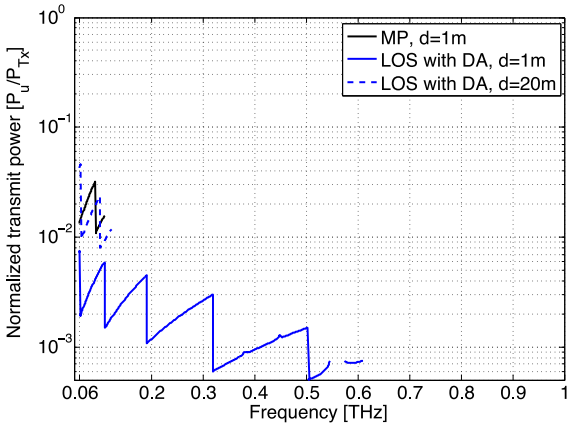

(a)

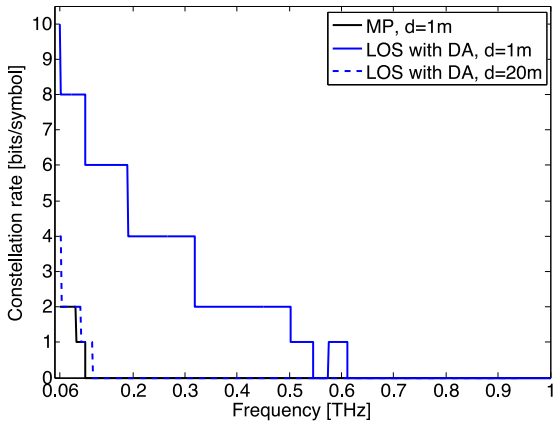

(b)

Fig. 5. Solution to the single-user resource allocation. (a) Transmit power. (b) Modulation rate.

A. Single-User THz Band Communication

1) Solution to the Resource Allocation: We obtain the numerical solutions to the developed optimization in (7), by using Algorithm 1. The initial value for the constant μ_1 is chosen as the maximum of the SINR values over the subwindows, which guarantees the feasibility of the solution. At each iteration, it is decreased by 5% (i.e., multiply with 0.95). A good value for the constant μ_2 is found via numerical search, and a general rule is that a smaller value is desired for a larger distance. In the resource allocation problem in (7), the transmit power and the modulation constellation are solved for the different transmission schemes over the different distances in Fig. 5(a) and (b), respectively.

Transmit Power: In the MP transmission (see Section II-B1), the normalized transmit power is shown for $d = 1$ m. The actual utilized BW is 0.06–0.11 THz. In the LOS with DA case (see Section II-B2), the transmit power allocation has the shape of a sawtooth, which is also observed in [12]. The utilized frequency bands are less than 0.61 THz. Being consistent with the spectral window analysis in Section II-B2, the path loss peak around 0.56 THz is avoided for transmission as shown in Fig. 5(a). When the distance increases to 20 m, the utilized frequency band shrinks to 0.12 THz. This can be explained that the SINR decreases as the distance or equivalently the path loss in the channel increases. In this case, the resource needs to be focused on the high SINR region, which lies in the lower THz band.

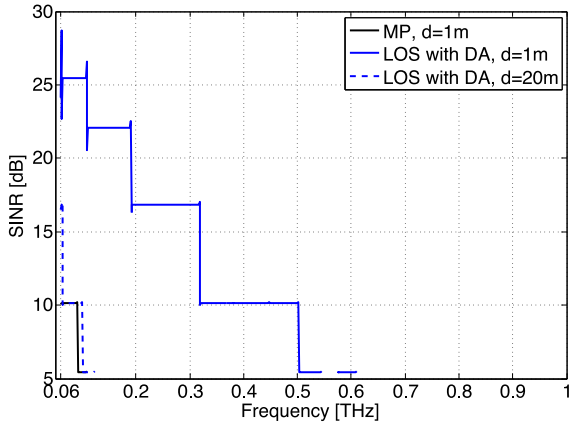

Fig. 6. SINR for the different transmission schemes.

Modulation Rate: At $d = 1$ m in the MP case, 2 b/symbol or 4-QAM is allocated for the 0.06–0.091 THz, while 1 b/symbol or BPSK is allocated for 0.091–0.11 THz, in our resource allocation model. On the contrary, for the same distance in the LOS with DA case, 10 b/symbol is supported from 0.06 to 0.061 THz, which implies the very high-order 1024-QAM. Then, smaller signal constellations are selected for higher carrier frequencies, due to their larger path loss values. When the distance is 20 m, the single-user data rate are approximated as 4 b/Hz $\cdot$ 3 GHz $+ 2$ b/Hz $\cdot$ 35 GHz $+ 1$ b/Hz $\cdot$ 20 GHz $= 102$ Gb/s.

2) SINR: The resulting SINR in (4) is evaluated in Fig. 6, with the obtained transmit power. We consider the IBI leakage of 17.47% to the neighboring subwindows, for the rectangular waveform G in (4). The nonzero SINR values appear when the subwindows are utilized. When $G_t = G_r = 20$ dBi and $d = 1$ m,10 b/symbol is supported and the SINR reaches 28 dB. Although at some utilized subwindows such as 0.5–0.55 and 0.57–0.61 THz, the SINR drops below the threshold 10 dB, the average BER requirement in (11) is satisfied. Interestingly, the fluctuations in the SINR occur when the constellation rate changes or equivalently, the transmit power changes sharply in the sawtooth shape, for example, at 0.061, 0.1, and 0.19 THz, among others. This is due to the sharp change of the transmit power at these frequencies, which make noticeable effects on the IBI in (3), and consequently, the fluctuations of SINR.

3) Distance Improvement: The resource allocation model is used to maximize the data rate in (7), while as the main objective, the distance maximization is then analyzed as shown in (5), for a given rate threshold R_{su}. The data rate performance for the MP with $G_t = G_r = 0$ dBi and the LOS with $G_t = G_r = 20$ dBi are illustrated in Fig. 7(a) and (b). For comparison, the water-filling capacity is an upper bound of the achievable data rates, while the equal-power capacity suggests the achievable data rates of the nonadaptive transmission.

MP with $G_t = G_r = 0$ dBi: In Fig. 7(a), the results based on the resource allocations scheme is significantly higher than the nonadaptive equal-power scheme. This advantage is more notable in the MP case since the intelligent allocation of the

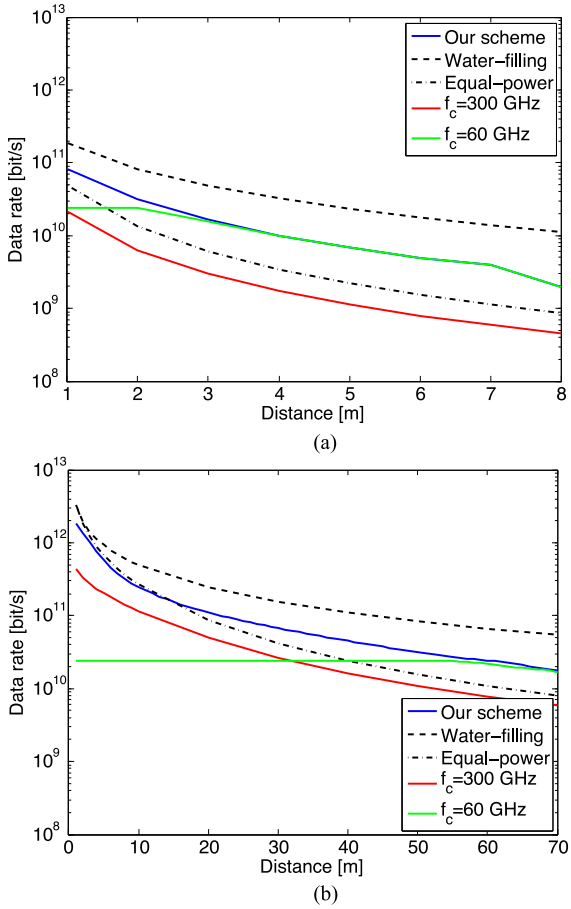

Fig. 7. Data rates in the single-user THz band communication. (a) MP with $G_t = G_r = 0$ dBi. (b) LOS with $G_t = G_r = 20$ dBi.

transmit power and the symbol constellation is more important when the channel quality is degraded. As discussed in Section II-B1, the path loss threshold sets the distance limit as 8 m. At 1 m, the data rate reaches 81.5 Gb/s. If $R_{\rm su} = 10$ Gb/s, the solution to the maximal distance in (5) is 4 m, which is greater than the results from the other schemes, such as 2.3 m of the equal-power scheme and 1.7 m of the 300 GHz system. Interestingly, the performance of the 60 GHz system is very close to our resource allocation scheme (operating over 0.06–1 THz), particularly when $d > 3$ m and the channel path loss is high. This can be explained since the resource is allocated to the lower frequency bands with better SINR, as discussed in Section V-A1.

LOS with $G_t = G_r = 20$ dBi: Fig. 7(b) shows that 1 Tb/s is achievable with our resource allocation scheme over the 0.06–1 THz band, up to $d = 3$ m, since the total usable BW is significantly enhanced with the use of the antenna gains [as shown in Section II-B2 and Fig. 2(b)]. When the distance is below 10 m, the SINR is very high over the subwindows. Consequently, the resource allocation plays less important role and its data rate is similar to the equal-power scheme. However, the advantage appears as the distance increases. If $R_{\rm su} = 100$ Gb/s, the solution to the maximal distance in (5) is 21 m. The significant distance improvement is obtained over the equal-power scheme, and the fixed BW system over 300 GHz, where the results of these two schemes are 17 and 10 m. With the high-gain antennas, the data rate of the 60 GHz system is flat and starts decreasing when the distance is above 60 m, since the SINR below 60 m is large enough to support the highest MQAM in the 60 GHz system.

Comparing to the 60 GHz system, when the distance is small, the advantage of our resource allocation using the 0.06–1 THz band is large, since much BW has high SINR and can be utilized. However, as the distance grows, the path loss drastically increases particularly for the high frequencies. The transmission resource is concentrated to the lower frequencies. In particular, when $d \geq 60$ m, the performances of the 60 GHz and the entire THz band have negligible difference.

4) Discussions: In our resource allocation scheme, the resource that includes the transmit power and the signal constellation are preferably distributed to the subwindows with lower frequencies or equivalently higher SINR. The advantage of our scheme becomes more important when the distance increases, compared with the fixed allocation scheme. By using the same resource allocation scheme to exploit the 0.06–1 THz band has the better performance over the millimeter-wave technologies at 60 and 300 GHz, particular when the distance is small. Furthermore, the distance improvement is significant with our resource allocation. In particular, 10 Gb/s can be supported at 4 m in the MP channel. On the other hand, 100 Gb/s is achieved up to 21 m in the LOS transmission with the use of 20-dBi gain antennas. In light of the spectrum utilization, the actual utilized BW is less than the total usable BW as in Fig. 2(b). Hence, the spectrum in the THz band is still under exploited in the single-user case. This further motivates the design of a strategic spectrum allocation for the multiuser network, as studied in Section IV-A.

B. Multiuser THz Band Communication Networks

We next evaluate the distance-aware BW-adaptive resource allocation scheme in a multiuser network in the THz band. Our optimization goal is to maximize the total distance of the ultrahigh-speed links, since we intend to support multiple links at the same time and address the distance challenge. Each link needs to reach the data rate greater than $R_{\rm mu}^{\rm th}$ in (28). First, we study the theoretical bounds and analyze the performance of the resource allocation scheme in the multiuser network, in terms of the data rate and the distance.

1) Theoretical Bounds Analysis: We start with link 1 with $d_1 = 21$ m, which is the largest distance that can support 100 Gb/s for LOS with $G_t = G_r = 20$ dBi, as studied in Section V-A3. We show that additional links can be concurrently supported by using the unused THz spectrum, without compromising the transmission of link 1. To allocate the second link using the unoccupied spectrum, we check the spectrum pool $\overrightarrow{SP}$ and apply the flowchart in Fig. 4. To analyze the theoretical bounds, we consider the two-user case and study the attainable data rate, R_2, while the higher number of multiuser networks can be extended by applying the same principle.

In Fig. 8(a) and (b), the link data rate in the multiuser network is no greater than that of the single-user link with the same distance, i.e., $R_{\rm mu}^2(d_2) \leq R_{\rm su}(d_2)$. The central part of the

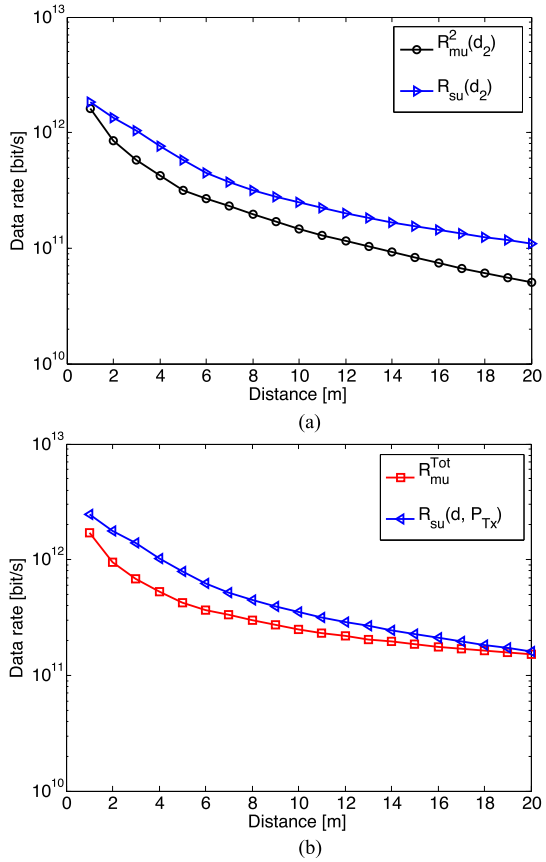

Fig. 8. Theoretical bounds in the multiuser THz band networks, for LOS with $G_t = G_r = 20$ dBi. (a) $R^i_{\mathrm{mu}}(d_i) \leq R_{\mathrm{su}}(d_i)$, with $I = 2$. (b) $R_{\mathrm{su}}(d_1) \leq R^{\mathrm{Tot}}_{\mathrm{mu}} \leq R_{\mathrm{su}}(d_I, I \cdot P_{\mathrm{Tx}})$, with $I = 2$.

spectrum is occupied by link 1 and cannot be used by link 2, which causes this data rate gap. Second, in Fig. 8(b), we observe that $R^{\mathrm{Tot}}_{\mathrm{mu}} \geq R_{\mathrm{su}}(d_1 = 21\mathrm{m}) = 102.4$ Gb/s, since the strategic allocation scheme provided in Section IV-A utilizes the spectrum resource more efficiently than the single-user case, since additional BW is used in the multiuser network support other links, without compromising the link 1.

Third, the results in Fig. 8(b) show that the multiuser data rate is bounded by $R_{\mathrm{su}}(d_2, 2P_{\mathrm{Tx}})$. The total usable BW is dependent on the shortest link in the network. In the single-user ($d = d_I$) and the multiuser cases, the total usable BW are equal. However, in the multiuser network, the centers of the spectral windows are occupied by long-distance links, which have higher path loss and consequently, worse rate performance. This results in the total multiuser data rate is less than the single-user rate, while the transmit power is calibrated as $I \cdot P_{\mathrm{Tx}}$ for the fair comparison. Furthermore, the advantage of $R_{\mathrm{su}}(d_2, 2P_{\mathrm{Tx}})$ decreases as the distance increases, maintaining greater than R_{mu}. This can be explained that the resource allocation scheme in the single-user communication optimizes the modulation and transmit power solutions. As for the data rate, we observe that $R_2 \geq 100$ Gb/s is reachable as long as $d_2 \leq 12$ m.

2) Multiuser Ultrahigh-Speed Network: We find the solution in (24) to maximize the total distance of ultrahigh-speed links in the multiuser network. By following the proposed strategic spectrum utilization principle in the flowchart (see Fig. 4), we iteratively allocate the spectrum to multiple users to satisfy the data rate requirement.

MP with $G_t = G_r = 0$ dBi: To start with, we set link 1 at $d_1 = 4$ m, which is the largest distance that supports $R^{\mathrm{th}}_{\mathrm{mu}} = 10$ Gb/s, as given in Section V-A3. Then, by exploiting the rest of the THz spectrum, link 2 is found at $d_2 = 3$ m as the largest distance to satisfy the rate requirement. By iterating this process, we obtain 14 links as provided inTable I. In each iteration, the maximal reachable distance that satisfies $R^{\mathrm{th}}_{\mathrm{mu}}$ is obtained, i.e., $\max d_{i+1}$ while $d_{i+1} \leq d_i$. This process iterates until we reach $d_{14} = 1$ m, when the remaining spectrum cannot support a link to exceed $R^{\mathrm{th}}_{\mathrm{mu}} = 10$ Gb/s. The number of utilized subwindows as well as the percentage of the total utilizable BW are also listed for each link. The overall network data rate in this analysis is 140 Gb/s, which is 13 times higher than the single-user rate with $d = 4$ m. The sum of the link distances in (24) is equal to 24 m. However, in this case, the utilized spectrum is between 0.06 and 0.2 THz.

LOS with $G_t = G_r = 20$ dBi: Similar process is applied in the LOS case with the high-gain antennas. To start with, we accommodate link 1 at $d_1 = 21$ m. Then, by inspecting the spectrum pool, the link 2 has $d_2 = 12$ m, which is the largest distance to support $R^{\mathrm{th}}_{\mathrm{mu}} = 100$ Gb/s transmission. The link information is summarized in Table I. Importantly, by applying the developed resource allocation scheme, 13 100 Gb/s links can be simultaneously supported in the THz band network. The overall network data rate reaches 1.31 Tb/s, which is 12 times higher than the single-user rate with $d = 21$ m. The sum of the link distances in (24) is equal to 71 m.

Moreover, the ultimate spectrum utilization is demonstrated in Fig. 9, where the constellation rate is shown as the function of the frequency for different links. The entire 0.06–1 THz spectrum is utilized, by using the developed strategic principle, which shows a significant improvement over the single-user case. Specifically, the spectrum between 0.06 and 1 THz is fully exploited, while only 60 subwindows as given in Table I (between 0.06 and 0.12 THz) are utilized for $d_1 = 21$ m. Moreover, the strategic spectrum allocation scheme developed in Section IV-A is applied and illustrated in Fig. 9, for example, for the links d_7, d_8, and d_9, over the spectrum around 0.6 THz. In particular, the central spectrum is allocated to d_7, while the outer subwindows are allocated to d_8 and then d_9, which have the lower path losses.

The percentage of the total utilizable BW [see Fig. 2(b)], which is the ratio between the utilized BW and the total utilizable BW at the particular distance, is also shown in Table I. With the smaller distance, the total utilizable BW grows, which results in a reduction of the percentage. However, for the same distance and for link i and $i + 1$, the percentage of the link $i + 1$ is greater or equal to that of the link i, since the better subwindows have already been selected for the link i. To achieve the same data rate $R^{\mathrm{th}}_{\mathrm{mu}}$, more subwindows are needed for the link $i + 1$. For example, this observation is supported in links 7 and 8 with the LOS communication over 3 m.

Comparison: We compare our resource allocation scheme with the nonadaptive scheme, in which the fixed frequency

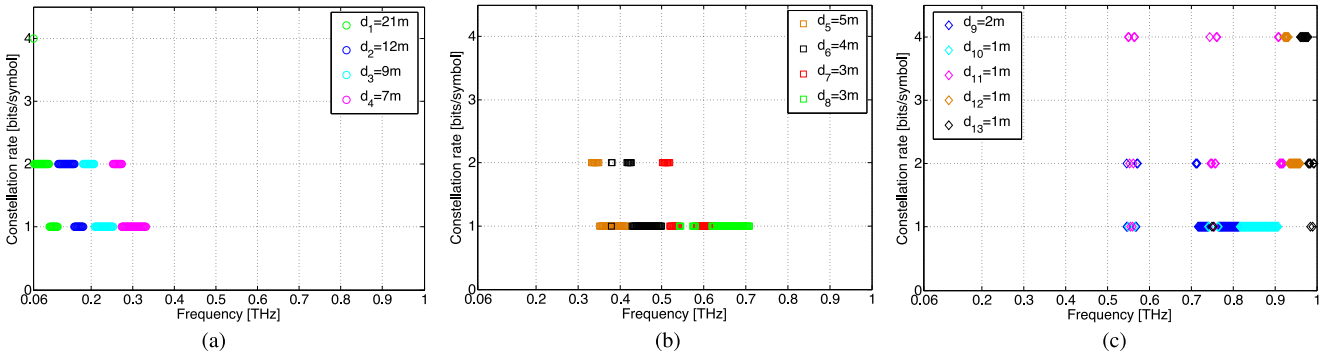

Fig. 9. Resource allocation solution in the multiuser network, for LOS with $G_t = G_r = 20$ dBi. (a) Links 1–4. (b) Links 5–8. (c) Links 9–13.

TABLE I
RESOURCE ALLOCATION SCHEME IN MULTIUSER NETWORKS

MP with $G_t = G_r = 0$ dBi: $R_{\rm mu}^{\rm th} = 10$ Gb/s														
Link number	1	2	3	4	5	6	7	8	9	10	11	12	13	14
Distance [m]	4	3	3	2	2	2	1	1	1	1	1	1	1	1
# of Utilized subwindows	10	10	10	10	10	10	10	10	10	10	10	10	10	10
% of Utilizable BW	15%	10%	10%	6%	6%	6%	3.4%	3.4%	3.4%	3.4%	3.4%	3.4%	3.4%	3.4%
LOS with $G_t = G_r = 20$ dBi: $R_{\rm mu}^{\rm th} = 100$ Gb/s														
Link number	1	2	3	4	5	6	7	8	9	10	11	12	13	
Distance [m]	21	12	9	7	5	4	3	3	2	2	1	1	1	
# of Utilized subwindows	60	61	73	80	82	87	82	101	91	101	33	39	39	
% of Utilizable BW	8.1%	7.1%	8.3%	8.9%	9%	9.5%	8.9%	10.9%	9.7%	10.7%	3.5%	4.1%	4.1%	

division, the equal transmit power, and the fixed modulation are adopted. In particular, 50 subwindows are assigned for each user, as suggested in [30]. The equal transmit power (i.e., $P_u = P_{\rm Tx}/50$) and the fixed 16-QAM modulation (i.e., $k_{\rm fixed} = 4$) that was designed for the THz system [32] are used on each subwindow. From (9), the resulting threshold SINR to support this transmission over each subwindow is given by

$$\gamma_{\rm th} = -\frac{(2^{k_{\rm fixed}} - 1)\ln(5\epsilon_{\rm th})}{1.5}. \tag{35}$$

However, this nonadaptive scheme supports the largest data rate of 92 Gb/s at $d = 1$ m, with only 23 subwindows satisfying the SINR requirement in (35).

3) Discussions: By using the developed strategic spectrum utilization principle and the resource allocation scheme in the multiuser case, the theoretical bounds of the multiuser data rate are evaluated. Moreover, the spectrum utilization is greatly improved using our scheme. In the MP channel, 14 links can be supported simultaneously with $R_{\rm mu}^{\rm th} = 10$ Gb/s, and the total distance over these links is 24 m. When the high-gain antennas are used for the LOS propagation, 13 100 Gb/s links can be supported simultaneously. The sum of the distances of these links reaches 71 m. The performance of the developed resource allocation scheme is significantly better than the nonadaptive system, due to the successful exploitation of the THz spectrum and the adaption of the transmit power and the modulation.

VI. CONCLUSION

In this paper, we developed a novel distance-aware BW-adaptive resource allocation scheme for THz band communication networks, with the objective to enhance the distance. The proposed scheme captures the unique channel peculiarities, and strategically utilizes the spectrum to enable multiple ultrahigh-speed links. Based on the developed scheme, we solved the solutions to the subwindows allocation, the modulation adaptation and the transmit power control in the resource allocation model, for both single-user and multiuser communications.

Recently, some millimeter-wave frequency bands (e.g., 71–76, 81–86, and 92–95 GHz) become licensed spectrum. On the one hand, the developed resource allocation scheme for the (0.06–10) THz band in this paper can be seamlessly applied by eliminating the regulated spectrum from the total usable BW [see Fig. 2(b)] if needed. On the other hand, the proposed solution in this paper can also benefit the millimeter-wave systems, by leveraging the concepts of cognitive radio networks [33]. For example, the proposed resource allocation scheme provides an efficient solution to utilize the regulated spectrum when the primary users are not present. These research directions will be investigated in the future work.

REFERENCES

[1] C. Han and I. F. Akyildiz, "Distance-aware multi-carrier (DAMC) modulation in terahertz band communication," in *Proc. IEEE Int. Conf. Commun.*, 2014, pp. 5461–5467.
[2] J. Federici and L. Moeller, "Review of terahertz and subterahertz wireless communications," *J. Appl. Phys.*, vol. 107, no. 11, 2010, Art. no. 111101.

[3] I. F. Akyildiz, D. M. Gutierrez-Estevez, R. Balakrishnan, and E. Chavarria-Reyes, "LTE-advanced and the evolution to beyond 4G (B4G) systems," *Phys. Commun.*, vol. 10, pp. 31–60, 2014.
[4] I. F. Akyildiz, J. M. Jornet, and C. Han, "TeraNets: Ultra-broadband communication networks in the terahertz band," *IEEE Wireless Commun.*, vol. 21, no. 4, pp. 130–135, Aug. 2014.
[5] T. Kürner and S. Priebe, "Towards THz communications-status in research, standardization and regulation," *J. Infrared Millim.* THz *Waves*, vol. 35, pp. 1–10, 2013.
[6] I. F. Akyildiz, J. M. Jornet, and C. Han, "Terahertz band: Next frontier for wireless communications," *Physical Commun.*, vol. 12, pp. 16–32, 2014.
[7] C. Han, A. O. Bicen, and I. F. Akyildiz, "Multi-ray channel modeling and wideband characterization for wireless communications in the terahertz band," *IEEE Trans. Wireless Commun.*, vol. 14, no. 5, pp. 2402–2412, May 2015.
[8] Z. Shen, J. G. Andrews, and B. L. Evans, "Adaptive resource allocation in multiuser OFDM systems with proportional rate constraints," *IEEE Trans. Wireless Commun.*, vol. 4, no. 6, pp. 2726–2737, Nov. 2005.
[9] W. Rhee and J. M. Cioffi, "Increase in capacity of multiuser OFDM system using dynamic subchannel allocation," in *Proc. IEEE Trans. Veh. Technol. Conf.*, 2000, vol. 2, pp. 1085–1089.
[10] Y. J. A. Zhang and K. B. Letaief, "An efficient resource-allocation scheme for spatial multiuser access in MIMO/OFDM systems,"*IEEE Trans. Commun.*, vol. 53, no. 1, pp. 107–116, Jan. 2005.
[11] K. B. Letaief and Y. J. Zhang, "Dynamic Multiuser resource allocation and adaptation for wireless systems," *IEEE Wireless Commun.*, vol. 13, no. 4, pp. 38–47, Aug. 2006.
[12] S. T. Chung and A. J. Goldsmith, "Degrees of freedom in adaptive modulation: A unified view," *IEEE Trans. Commun.*, vol. 49, no. 9, pp. 1561–1571, Sep. 2001.
[13] J. M. Jornet and I. F. Akyildiz, "Femtosecond-long pulse-based modulation for terahertz band communication in nanonetworks," *IEEE Trans. Commun.*, vol. 62, no. 5, pp. 1742–1754, May 2014.
[14] C. Han, A. O. Bicen, and I. F. Akyildiz, "Multi-wideband waveform design for distance-adaptive wireless communications in the terahertz band," *IEEE Trans. Signal Process.*, vol. 64, no. 4, pp. 910–922, Feb. 2016.
[15] S. Koenig *et al.*, "Wireless sub-THz communication system with high data rate," *Nature Photon.*, vol. 7, no. 12, pp. 977–981, 2013.
[16] A. J. Seeds, H. Shams, M. J. Fice, and C. C. Renaud, "Terahertz photonics for wireless communications," *J. Lightw. Technol.*, vol. 33, no. 3, pp. 579–587, Feb. 2015.
[17] S. Koenig *et al.*, "Wireless sub-THz communication system with high data rate enabled by RF photonics and active MMIC technology," in *Proc. IEEE Photon. Conf.*, 2014, pp. 414–415.
[18] J. M. Jornet and I. F. Akyildiz, "Channel modeling and capacity analysis for electromagnetic wireless nanonetworks in the terahertz band," *IEEE Trans. Wireless Commun.*, vol. 10, no. 10, pp. 3211–3221, Oct. 2011.
[19] T. Schneider, A. Wiatrek, S. Preußler, M. Grigat, and R.-P. Braun, "Link budget analysis for terahertz fixed wireless links," *IEEE Trans.* THz *Sci. Technol.*, vol. 2, no. 2, pp. 250–256, Mar. 2012.
[20] I. C. Wong and B. L. Evans, *Resource Allocation in Multiuser Multicarrier Wireless Systems*. Berlin, Germany: Springer-Verlag, 2008.
[21] J. M. Jornet and I. F. Akyildiz, "Graphene-based plasmonic nano-antenna for terahertz band communication in nanonetworks," *IEEE J. Sel. Areas Commun.*, vol. 31, no. 12, pp. 685–694, Dec. 2013.
[22] M. Tamagnone, J. Gomez-Diaz, J. Mosig, and J. Perruisseau-Carrier, "Analysis and design of terahertz antennas based on plasmonic resonant graphene sheets," *J. Appl. Phys.*, vol. 112, no. 11, 2012, Art. no. 114915.
[23] L. Vicarelli *et al.*, "Graphene field-effect transistors as room-temperature terahertz detectors," *Nature Mater.*, vol. 11, pp. 865–871, 2012.
[24] J. M. Jornet and I. F. Akyildiz, "Graphene-based plasmonic nano-transceiver for terahertz band communication," in *Proc. IEEE 8th Eur. Conf. Antennas Propag.*, 2014, pp. 492–496.
[25] R. C. Daniels and R. W. Heath, "60 GHz wireless communications: Emerging requirements and design recommendations," *IEEE Veh. Technol. Mag.*, vol. 2, no. 3, pp. 41–50, Sep. 2007.
[26] W. D. Wu, C. C. Lee, C. H. Wang, and C. C. Chao, "Signal-to-interference-plus-noise ratio analysis for direct-sequence ultra-wideband systems in generalized Saleh–Valenzuela channels," *IEEE J. Sel. Topics Signal Process.*, vol. 1, no. 3, pp. 483–497, Oct. 2007.
[27] C. Y. Wong, R. S. Cheng, K. B. Lataief, and R. D. Murch, "Multiuser OFDM with adaptive subcarrier, bit, and power allocation," *IEEE J. Sel. Areas Commun.*, vol. 17, no. 10, pp. 1747–1758, Oct. 1999.
[28] S. Falahati, A. Svensson, T. Ekman, and M. Sternad, "Adaptive modulation systems for predicted wireless channels," *IEEE Trans. Commun.*, vol. 52, no. 2, pp. 307–316, Feb. 2004.
[29] T. Keller and L. Hanzo, "Adaptive multicarrier modulation: A convenient framework for time-frequency processing in wireless communications," *Proc. IEEE*, vol. 88, no. 5, pp. 611–640, May 2000.
[30] S. Priebe, M. Kannicht, M. Jacob, and T. Kurner, "Ultra broadband indoor channel measurements and calibrated ray tracing propagation modeling at Thz frequencies," *IEEE J. Commun. Netw.*, vol. 15, no. 6, pp. 547–558, Dec. 2013.
[31] T. Rappaport, J. Murdock, and F. Gutierrez, "State of the art in 60-GHz integrated circuits and systems for wireless communications," *Proc. IEEE*, vol. 99, no. 8, pp. 1390–1436, Aug. 2011.
[32] C. Wang *et al.*, "0.34-Thz wireless link based on high-order modulation for future wireless local area network applications," *IEEE Trans. THz Sci. Technol.*, vol. 4, no. 1, pp. 75–85, Jan. 2014.
[33] I. F. Akyildiz, W.-Y. Lee, M. C. Vuran, and S. Mohanty, "Next generation/dynamic spectrum access/cognitive radio wireless networks: A survey," *Comput. Netw.*, vol. 50, no. 13, pp. 2127–2159, 2006.

Chong Han (M'16) received the Bachelor of Engineering degree in electrical engineering and telecommunications from the University of New South Wales, Sydney, NSW, Australia, in 2011, and the Master of Science and Ph.D. degrees in electrical and computer engineering from the Georgia Institute of Technology, Atlanta, GA, USA, in 2012 and 2016, respectively.

He is currently an Assistant Professor with the University of Michigan–Shanghai Jiao Tong University Joint Institute, Shanghai Jiao Tong University, Shanghai, China. His research interests include THz band communication networks, 5G cellular networks, electromagnetic nanonetworks, and graphene-enabled wireless communications.

Ian F. Akyildiz (M'86–SM'89–F'96) received the B.S., M.S., and Ph.D. degrees in computer engineering from the University of Erlangen–Nurnberg, Erlangen, Germany, in 1978, 1981, and 1984, respectively.

He is currently the Ken Byers Chair Professor of telecommunications with the School of Electrical and Computer Engineering, Georgia Institute of Technology, Atlanta, GA, USA, the Director of the Broadband Wireless Networking Laboratory, and the Chair of the Telecommunication Group at the Georgia Tech. He is an honorary Professor with the School of Electrical Engineering at the Universitat Politecnica de Catalunya, Barcelona, Spain, and founded the NaNoNetworking Center, Catalunya, Spain. Since September 2012, he has been a Finland Distinguished Professor Program Professor supported by the Academy of Finland with the Department of Communications Engineering, Tampere University of Technology, Tampere, Finland. He is the Editor-in-Chief of *Computer Networks Journal*, and the founding Editor-in-Chief of the *Ad Hoc Networks* journal, the *Physical Communication* journal, and the *Nano Communication Networks* journal. His research interests include THz band communication, nanonetworks, software-defined networking, 5G cellular systems, and wireless underground sensor networks.

Dr. Akyildiz has been an ACM Fellow since 1997. He was the recipient of numerous awards from the IEEE and ACM.